Journal of Machine Construction and Maintenance
QUARTERLY ISSN 1232-9312 3/2018(110)

p. 57–69

Andrzej KUREK[a], Marta KUREK[a], Justyna KOZIARSKA[a], Sabrina VANTADORI[b], Tadeusz ŁAGODA[a, *]
[a] Opole University of Technology, Faculty of Mechanical Engineering, Opole, Poland
[b] Department of Engineering & Architecture, University of Parma, Italy
[*] Corresponding author: lagoda@po.opole.pl

FATIGUE CHARACTERISTICS OF 6082-T6 ALUMINIUM ALLOY OBTAINED IN TENSION-COMPRESSION AND OSCILLATORY BENDING TESTS

Key words: uniaxial loading, tension-compression, plane bending, plastic strain, fatigue.

Abstract: The paper presents the comparison of the results of experimental fatigue tests for 6082-T6 aluminium alloy, carried out for two states of loading: strain controlled tension-compression, and strain and bending moment controlled oscillatory bending. The following were used for that purpose: the Manson-Coffin-Basquin, Kandil, Langer, and the authors' own strain fatigue characteristics, and also the Basquin stress fatigue characteristic. Our experimental studies and adequate physical relationships were applied to convert the amplitudes of stress and strain occurring in rods without a geometrical notch subject to bending, according to the model of an elasto-plastic body. The obtained results were used to compare both loading types under different control methods and different fatigue characteristics.

Charakterystyki zmęczeniowe aluminium 6082-t6 uzyskane w próbie rozciagania-ściskania i whadadłowego zginania

Słowa kluczowe: obciążenie jednoosiowe, rozciąganie-ściskanie, zginanie w płaszczyźnie, odkształcenie plastyczne, zmęczenie.

Streszczenie: W pracy przedstawiono porównanie wyników eksperymentalnych prób zmęczeniowych dla stopu aluminium 6082-T6, przeprowadzonych dla dwóch stanów obciążenia: rozciąganie-ściskanie i ściskania oraz zginania oscylacyjnego kontrolowanego pod wpływem odkształcenia i zginania. Do tego celu użyto następujących parametrów: odkształceniowej charakterystyki zmęczeniowej Mansona-Coffina-Basquina, Kandila, Langera i autorów, a także naprężeniowej charakterystyki zmęczeniowej Basquina. Własne badania eksperymentalne i odpowiednie związki fizyczne zostały zastosowane do konwersji amplitud naprężenia i odkształcenia występującego w elementach zginanych bez karbu geometrycznego, zgodnie z modelem ciała sprężysto-plastycznego. Uzyskane wyniki wykorzystano do porównania obu typów obciążeń przy różnych metodach sterowania i różnych charakterystyk zmęczeniowych.

NOMENCLATURE

A, m – constants in the regression model,
b – fatigue life exponent,
c – exponent of plastic fatigue strain,
E – the Young's modulus,
K' – cyclic strength coefficient,
n' – cyclic strengthening exponent,
N_f – fatigue life in cycles,
$2N_f$ – the number of loading reversals (semi-cycles),
R – maximum height (radius in the case of round component /rod/),
x – the distance from bending plane,
$\varepsilon_{a,t}$ – total strain amplitude expressed as the sum of the amplitudes of elastic strain $\varepsilon_{a,e}$ and plastic strain $\varepsilon_{a,p}$,
e'_f – coefficient of plastic fatigue strain,
s'_f – fatigue life coefficient,
σ_a – stress amplitude for tension-compression or bending.

Introduction

The subject of material fatigue is an important issue in our economy every day. The effects of tension and bending are known virtually in each branch of industry; therefore, it is not a surprise that these two loading states are also considered with reference to material fatigue [1–3]. The majority of current fatigue characteristics are developed in tension-compression conditions. Unfortunately, this state of loading is very rare in real mechanical structures subject to fatigue loads [4]. Variable bending occurs more often [5]. As a result of this, the relation between fatigue characteristics for tension-compression and oscillatory bending constitutes an interesting and up-to-date subject for considerations [6]. It should be emphasised here that, in the case of bending, these characteristics are most often developed using the model of a perfectly elastic body.

This paper compares the characteristics of tension-compression and oscillatory bending for the model of a perfectly elastic and elasto-plastic body, using the models of stress and strain characteristics [7–9]. The analysis has been performed on the basis of fatigue tests completed for 6082-T6 aluminium alloy in the two considered loading states. The aim of this paper is to find a relevant difference between the fatigue life of aluminium alloy subjected to different states of loading and also finding a way to recalculate results from one state to another. It has been proven that, in the case of the elasto-plastic body model, fatigue life described by characteristics obtained for oscillatory bending is often higher than that for tension-compression. This shows that it is not ideal, but safe, to use conventional tension-compression characteristic to calculate the fatigue life of structures subject to oscillatory bending.

When analysing the issue of tension-compression, it is appropriate to begin with the Manson-Coffin-Basquin model (**MCB**) [10–12]:

$$\varepsilon_{a,t} = \varepsilon_{a,e} + \varepsilon_{a,p} = \frac{\sigma'_f}{E}\left(2N_f\right)^b + \varepsilon'_f\left(2N_f\right)^c \quad (1)$$

where
$\varepsilon_{a,t}$ – total strain amplitude expressed as the sum of the amplitudes of elastic strain $\varepsilon_{a,e}$ and plastic strain $\varepsilon_{a,p}$,
$2N_f$ – the number of loading reversals,
E – the Young's modulus,
s'_f, b – fatigue life coefficient and exponent,
e'_f, c – coefficient and exponent of fatigue plastic strain.

The original **MCB** characteristic has been developed for tension-compression while analysing the strain, stress, and the number of cycles until failure.

Model (1) is used only in the case when it is possible to determine separately both the elastic ε_{ae} and plastic ε_{ap} component of total strain ε_{at} [13, 14].

Then, for cyclic loading we obtain the following:

$$\varepsilon_{ae} = \frac{\sigma_a}{E} \quad (2)$$

and

$$\varepsilon_{ap} = \varepsilon_{at} - \varepsilon_{ae} \quad (3)$$

This relation is defined by the Ramberg-Osgood equation [15]:

$$\varepsilon_{a,t} = \varepsilon_{a,e} + \varepsilon_{a,p} = \frac{\sigma_a}{E} + \left(\frac{\sigma_a}{K'}\right)^{\frac{1}{n'}} \quad (4)$$

where
σ_a – stress amplitude,
K' – cyclic strength coefficient,
n' – cyclic strengthening exponent.

In 1910, Basquin [10] proposed the fatigue plot showing the relation between the number of cycles until failure and stress amplitude in a double-logarithmic system $\log(\sigma_a)\log(N_f)$, and the approximating formula, which can be expressed as below in the exponential form for tension-compression:

$$\sigma_a = \sigma'_f\left(2N_f\right)^b \quad (5)$$

or

$$\log N_f = A - m\log\sigma_a \quad (6)$$

where
N_f – fatigue life in cycles,
σ_a – stress amplitude for tension-compression or bending,
A, m – regression model constants.

Another issue has been shown in the study [14], where it is pointed out that the sense of plastic strain amplitude in the expression (1) depends on fatigue life, and thus c is not a constant value.

Moreover, various authors proposed another empirical model making total strain amplitude dependent on the number of cycles. Among these models, there is the Langer [16] proposal, which is used in numerous studies and promoted, e.g., by Manson [12, 17] and Chopra [18].

$$logN_f = A - B\,log(\varepsilon_{ac} - C) \quad (7)$$

where A, B, C – constants to select special form of the characteristic for a given material.

Another model is proposed by Kandil [19] and Gorash [20], in the following form:

$$log\varepsilon_{ac} = A - B\,log\left(N_f\right) + C\,log^2\left(N_f\right) \quad (8)$$

where A, B, C – constants to select special form of the characteristic for a given material.

Since, in the case of bending, it is not possible to separate elastic and plastic components, then Equation (1) cannot be used, but it is possible to use models (7) or (8), or another empirical form of a strain-life curve model. For example, this may be a combination of Equations (7) and (8) in the following form:

$$log(\varepsilon_{ac} - D) = A - B\,log(N_f) + C\,log^2(N_f) \tag{9}$$

where A, B, C, D – constants to select special form of the characteristic for a given material.

All the constants in models (7)–(9) are obtained according to ASTM standards, using least-squares method.

An extensive review of fatigue-life models can be found, e.g., in the studies [21] or [22]. The new form, which is proposed there, requires 4 material constants to be determined, which is the same as for the popular characteristic MCB (1).

In the literature, there is no simple model allowing the determination of elasto-plastic strains and stresses for smooth rods at bending. However, it has been confirmed empirically many times that normal strain distribution for bending is linear in cross-section:

$$\varepsilon_a(x) = \varepsilon_{a\,max}\,\frac{x}{R} \tag{10}$$

where x – the distance from bending plane, R – maximum height (radius in the case of round component /rod/).

The basic relationship that has to be satisfied is that normal stresses, which appear both in elastic and elasto-plastic models, must compensate the preset bending moment, which is expressed as the following:

$$M_b = \int_S \sigma(x, y)\,x\,dS \tag{11}$$

while the relationship between stress and strain amplitude may be expressed using the Ramberg-Osgood Equation (4). Figure 1 shows an example of the distribution of stresses and strains at bending.

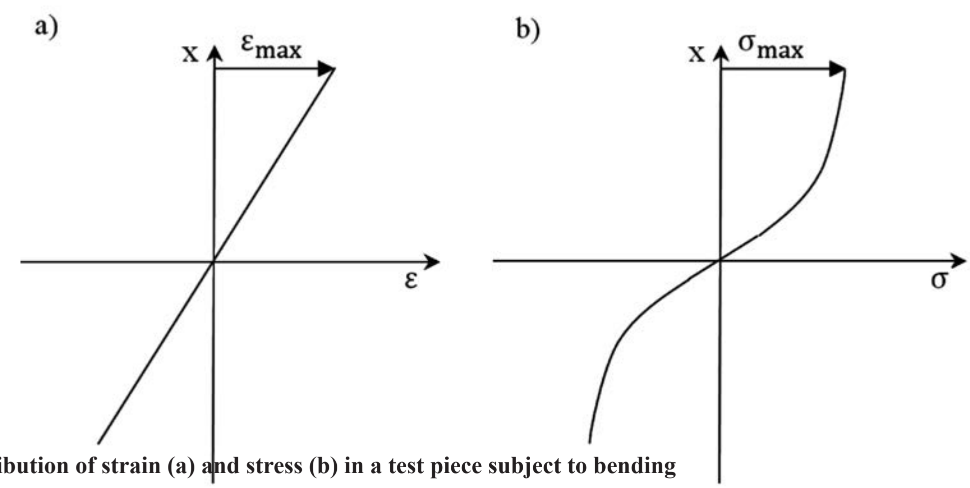

Fig. 1. Distribution of strain (a) and stress (b) in a test piece subject to bending

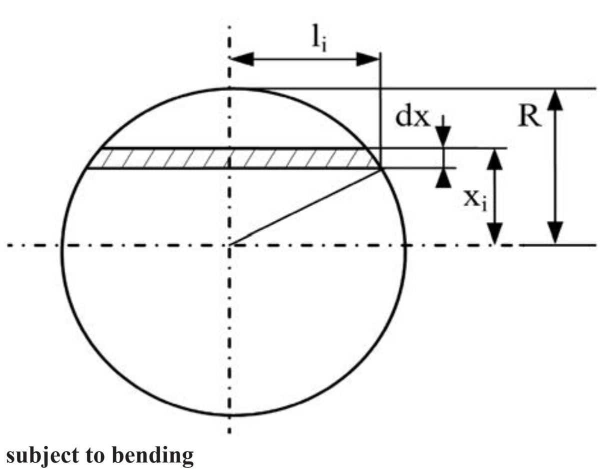

Fig. 2. Cross-section of test piece subject to bending

Figure 2 shows values in the test piece cross-section, required to calculate distributions of stresses and bending moment according to the elasto-plastic body model.

It should be noted that the static and fatigue Young's modulus can differ. Due to lack of characteristic value for fatigue Young's modulus, the static one was used for calculations.

1. Experimental studies

The studies were carried out for test pieces made of 6082-T6 material, an alloy, which is also known under other names (Table 1).

The chemical constitution of the tested material, according to the supplier, is shown in Table 2, and the basic mechanical properties measured by the authors are specified in Table 3.

Table. 1. Symbols of the 6082 aluminium alloy according to various standards (equivalents)

Standard	DIN	ISO	PN	Werkstoff	EN
Symbol	AlMgSi1	AlSi1MgMn	PA4	3.2315	6082

Table 2. Chemical constitution of 6082 aluminium alloy (in %)

Cu	Mg	Mn	Si	Fe	Zr+Ti	Zn	Cr
<0.1	0.6–1.2	0.4–1.0	0.7–1.3	<0.5	<0.1	<0.2	<0.25

Table 3. The basic mechanical parameters of 6082 aluminium alloy

$\sigma_{y,0.2}$, MPa	UTS, MPa	$A_{12.5}$ %	ν
365	385.2	27.2	0.32

The low-cycle tests for tension-compression were performed in cooperation with the Institute Laboratory for Materials and Structures Testing at UTP - University of Science and Technology in Bydgoszcz [23].

Fatigue tests for oscillatory bending were carried out using fatigue-testing machines belonging to the laboratory of the Department of Mechanics and Machine Design at Opole University of Technology.

2. Tests for tension-compression

The purpose of tests was to find basic fatigue characteristics for test pieces made of aluminium alloy at ambient temperature. After analysis of static tension test results, it was decided that the low-cycle tests would be carried out on five levels of total strain amplitude ε_{ac}: ε_{ac1}=0.35%, ε_{ac2}=0.5%, ε_{ac3}=0.8%, ε_{ac4}=1.0%, ε_{ac5}=2.0%

a)

b)

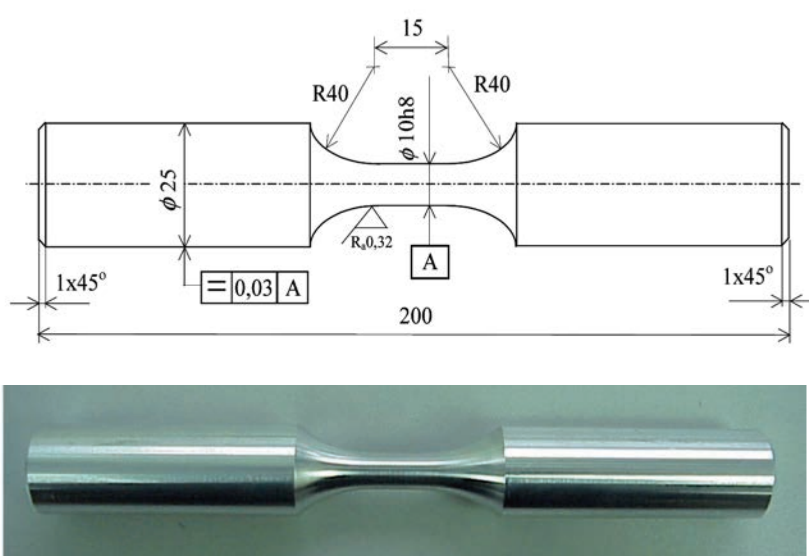

Fig. 3. The shape and dimensions of test pieces used in the tests: a) drawing with dimensions, in mm, b) test piece view

for a frequency of *f*=0.2 Hz and a strain ratio of R = - 1, and an extensometer was used to measure strain level.

In order to determine the levels of strain reached in conditions of low-cycle tests, they were preceded by the static tension test. A test piece for fatigue tests was used for that purpose (Fig. 3).

16 test pieces were used in the tests. The tests were performed according to the standard PN-84/H-04334.

The results of fatigue tests at single-axis tension-compression are compared in Table 4, where (e-p) stands for elasto-plastic. Material constants appearing in the Manson-Coffin-Basquin and Ramberg-Osgood characteristics have been determined on the basis of these results. These values are compared in Table 5.

The majority of materials are not cyclically stable. In the case of aluminium alloys, in general, we deal with their weakening. Fig. 4 shows the change in stresses at constant strain amplitude in the case of tension-compression.

Table 4. Fatigue test results for tension-compression at controlled strain amplitude for the 6082-T6 alloy

$\varepsilon_{a(e-p)}$, -	$\sigma_{a(e-p)}$, MPa	N_f, cycles
0.02	392.8	31
0.02	401.08	27
0.02	402.54	31
0.01	362.74	143
0.01	358.47	137
0.01	372.48	123
0.008	355.48	285
0.008	357.71	277
0.008	341.78	397
0.005	329.23	3101
0.005	337.07	2201
0.005	335.41	1881
0.0035	252.93	15766
0.0035	248.85	25951
0.0035	249.3	23241

Table 5. Cyclic parameters of the 6082-T6 aluminium alloy

K', MPa	n'	E, MPa	σ'_f, MPa	ε'_f	b	c
616	0.099	76998	533	0.185	-0.0656	-0.634

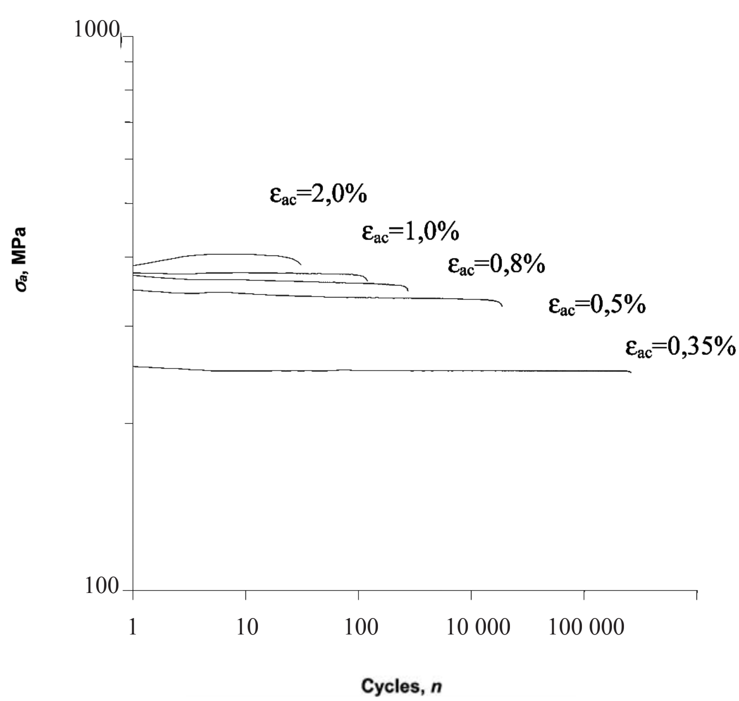

Fig. 4. Changes in hysteresis loop parameters on five strain levels: σ_a=f(*n*)

3. Tests for oscillatory bending

The “diabolo” type cylindrical test pieces without a geometrical notch were used in fatigue tests. The geometry of test pieces used results from the simplified localisation of spot characterised by highest stresses, and they are shown in Fig. 5. The starting material was a round rod made of the 6082-T6 alloy, ϕ16mm in diameter. The tests in cyclic conditions under controlled moment involved using 25 test pieces, and under controlled strain, 25 test pieces were used as well.

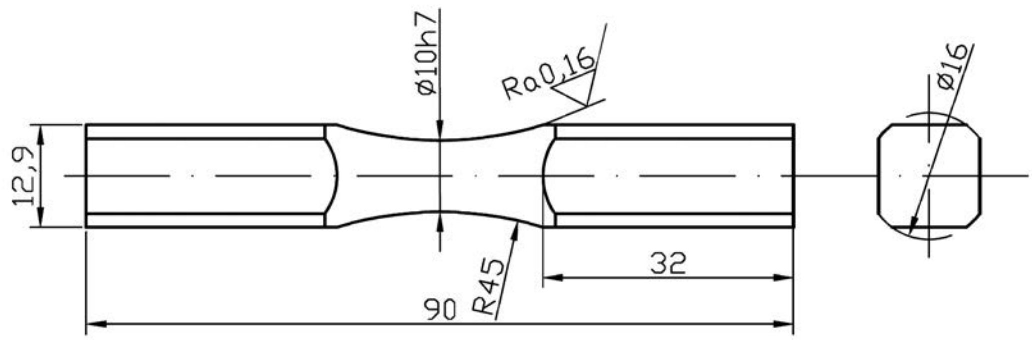

Fig. 5. The shape and dimensions of a test piece for fatigue tests

The cyclic (constant-amplitude) tests were carried out on a MZGS-100 test bench designed by Achtelik. Fig. 6 shows the view of a fatigue-testing machine. The MZGS-100 test bench consists of a propulsion system, head, loading system, and the control and measurement setup. The trajectory of bending moment M_g loading the test piece was the parameter monitored during the tests.

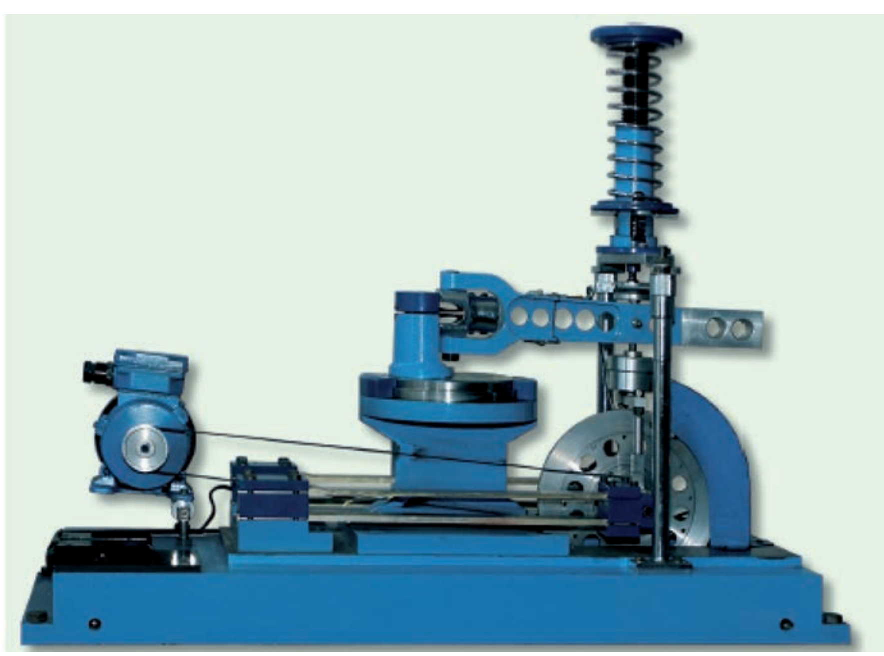

Fig. 6. The setup for fatigue tests under controlled moment

The results of tests under controlled moment converted into nominal values are compared in Table 6, where (e-p) stands for elasto-plastic, (a,n) nominal. Moreover, the table compares calculated stress and strain amplitudes for an elasto-plastic body model according to the previous description (eqs. 4,10, and 11).

Table 6. The results of fatigue tests for oscillatory bending under controlled moment for the 6082-T6 alloy

$\sigma_{a,n}$, MPa	$\sigma_{a(e-p)}$, MPa	$\varepsilon_{a(e-p)}$, -	N_f, cycles
195	194	0.00253	221000
195	194	0.00253	165700
195	194	0.00253	347700
168	167	0.00217	1536500
168	167	0.00217	774300
168	167	0.00217	586800
163	162	0.00211	2468700
164	163	0.00212	2585400
166	165	0.00214	552700
207	206	0.00269	105700
208	207	0.0027	113700
208	207	0.0027	84400
167	166	0.00216	571100
171	170	0.00221	449400
222	220	0.00289	353000
306	283	0.00405	4200
306	283	0.00405	5930
358	310	0.00497	2140
278	266	0.00365	17500
252	246	0.00329	38300
253	247	0.0033	39620
286	271	0.00376	7700
319	292	0.00428	8600
214	212	0.00277	118986
195	194	0.00253	130800

Fig. 7. The setup for fatigue tests under controlled strain

Fatigue tests under controlled strain were performed using a new setup shown in Fig. 7. In this case, lever excursion amplitude was controlled (fixed), which ensures a fixed strain amplitude on the test piece. Fatigue test results are compared in Table 7. Moreover, the table compares corresponding values of stress amplitudes according to the Ramberg-Osgood equation.

Table 7. The results of fatigue tests for oscillatory bending under controlled strain amplitude for the 6082-T6 alloy

$\varepsilon_{a(s-p)}$, -	$\sigma_{a(s-p)}$, MPa	N_f, cycles
0.00642	337	8684
0.00642	337	4489
0.00642	337	5591
0.00564	320	18599
0.00564	320	18873
0.00564	320	15770
0.00494	310	30000
0.00494	310	26766
0.00423	290	39728
0.00423	290	44280
0.00423	290	39000
0.00353	260	116400
0.00353	260	447170
0.00353	260	59573
0.00353	260	121400
0.00282	214	>2000000
0.00317	239	>2000000
0.00705	344	3500
0.00719	345	4000
0.00821	355	1500
0.00881	360	949
0.00917	363	1048
0.0098	367	650
0.01058	372	540

Fig. 8. An example test piece photo taken after oscillatory bending test

In the case of fatigue tests carried out both under controlled moment and strain, the instant when crack became visible with bare eyes (ca. 1 mm) was taken as fatigue life. Fig. 8 presents a typical test piece cross-section after oscillatory bending. In this photo, we can clearly see the initiation point and neutral plane in relation to which bending has been occurring.

Figure 9 demonstrates the change in bending moment amplitude during tests for a given strain amplitude. Moreover, the illustration allows reading off the instant of fatigue crack initiation, when the moment starts to drop rapidly. In our experiment, a fixed amount of bending moment amplitude drop (by 15%) was considered as crack initiation.

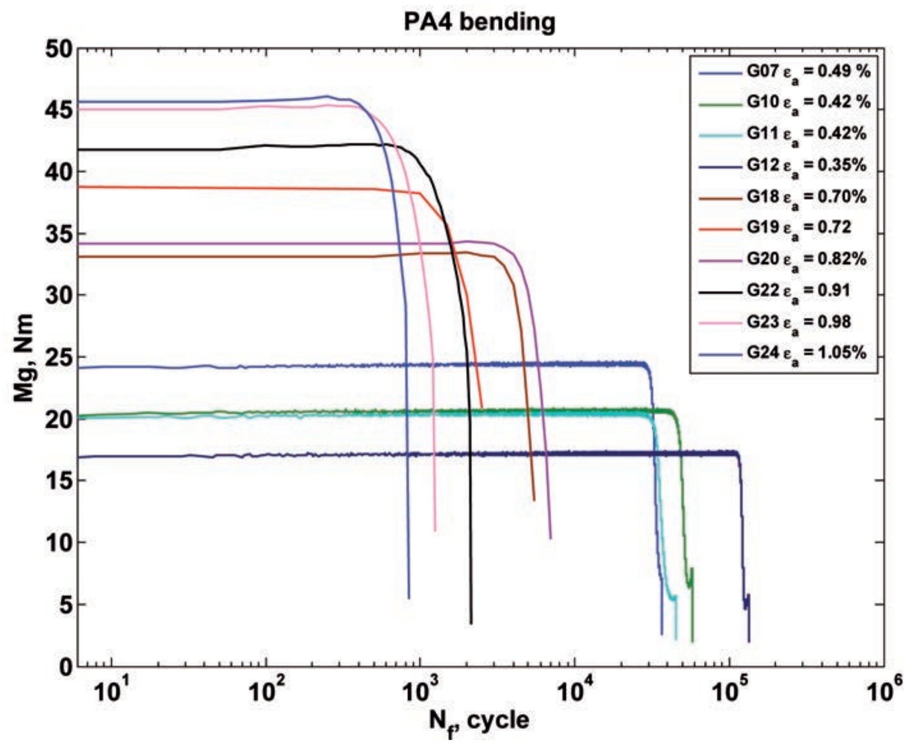

Fig. 9. Change in the moment depending on current number of cycles, in relation to strain amplitude

4. Comparison of test results

Completed tests and respective calculations provided grounds for determining fatigue characteristics, cumulatively shown in the illustrations. Constants appearing in the formulae are compared in successive tables. In the first place, the Basquin fatigue characteristics in form of (6) were determined. Fig. 10 and Table 8 compare the results of completed calculations. Fig. 10 shows that, when an elastic body model is chosen, the results of tests involving moment (stress) control are above those for the elasto-plastic body model. The other results for bending are very close. The characteristic for tension-compression looks slightly different; although, it has been determined for smaller range of cycles. Moreover, Fig. 10 shows cumulative characteristics for all analysed data taking into account material plasticity. However, it should be noted that, for the life range of 20 - $2 \cdot 10^6$ cycles, it is not right to choose a straight line. The shape of this diagram is more like the letter S, as mentioned, e.g., in the study [24].

The model of stress fatigue characteristics proposed in this study is intended to describe the tests involving low and high number of cycles.

$$\log \frac{\sigma_a}{R_m} = B \log 2N_f + C\, log^2(2N_f) \quad + D\, log^3(2N_f) \tag{12}$$

where
σ_a – stress amplitude,
$2N_f$ – the number of loading recurrences (semi-cycles),
R_m – tensile strength
B, C, D – constants.

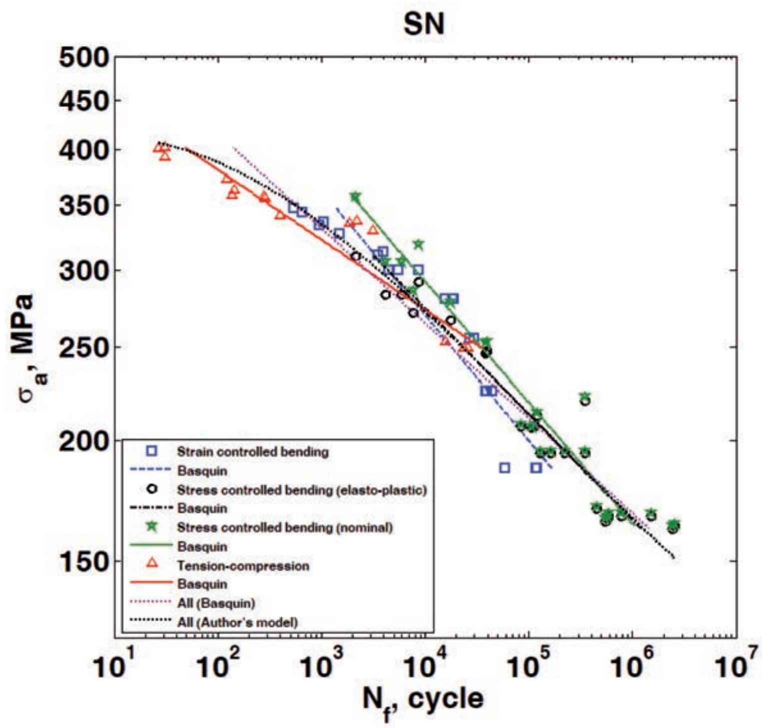

Fig. 10. Fatigue characteristics according to the Basquin and Authors' models (eq. 9)

Table 8. Comparisons of parameters of the analysed characteristics according to stress models by Basquin and Authors

Basquin			
		A	m
bending nominal (stress controlled)		23.7053	7.993
bending elasto-plastic (stress controlled)		26.2529	9.1287
bending (strain controlled)		22.7567	7.7175
Tension-compression		37.5945	13.7902
All (elasto-plastic)		28.6698	10.1849
Authors' model			
	B	**C**	**D**
All (elasto-plastic)	0.05798	-0.03226	0.002079

Successive analyses concern strain characteristics. The Manson-Coffin-Basquin characteristic (1) was the first one to be analysed. Analysis of Fig. 11 and Table 9 allows observing that, in practice, all three observed characteristics overlap and it is possible to find one cumulative characteristic. However, it should be noted that, in the case of bending, the MCB characteristic can be determined only due to the previously defined Ramberg-Osgood characteristic (4), which allows separating elastic and plastic components of strain. Considering this, it seems necessary to seek other characteristics where there is no need to divide strain into an elastic and plastic components. Finding such a model will allow determining fatigue characteristics under controlled strain at bending on relatively simple and inexpensive machines.

The Langer characteristic (7) was employed first. It is the simplest one, and originally it assumes a linear character in a double-logarithmic system. Fig. 12 compares these characteristics for individual tests. Parameters of these characteristics are presented in Table 10. Completed data analysis indicates that the characteristic for tension-compression and the cumulative characteristic approximate the empirical data incorrectly. As a result of this, it cannot be used for the correct description of the empirical data. The Kandil characteristic (8) was taken as the second one. It is more complex than the Langer characteristic, and, as it may be concluded from Fig. 13 and data collected in Table 11, it describes experimental test results by far better. This applies both to the description of these results for individual tests and the cumulative characteristic determined for all tests. The last characteristic used is the one proposed by the authors of this study in form of (9). Another, fourth parameter to be determined appears in this characteristic. Analysis of Fig. 14 and data contained in Table 12 proves that, as in the case of the Langer characteristic, this characteristic describes all test results very well, both individually and for all tests jointly. Analysis of correlation coefficients for all three analysed strain characteristics (Tables 10, 11 and 12) indicates that the best match of combined characteristics is ensured in the case of the model proposed by the authors of this study.

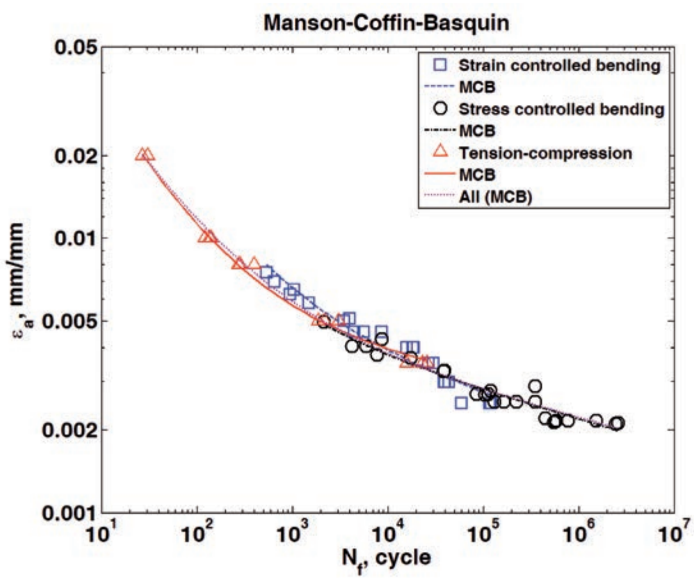

Fig. 11. Fatigue characteristics according to the Manson-Coffin-Basquin model

Table 9. Comparison of parameters of the analysed characteristics according to the Manson-Coffin-Basquin model

Manson-Coffin-Basquin				
	b	***c***	***s'$_f$*, *MPa***	***e'$_f$***
bending (stress controlled)	-0.1014	-0.6566	733.4613	0.1876
bending (strain controlled)	-0.1127	-0.6359	823.0734	0.2755
Tension-compression	-0.0656	-0.6340	533.2891	0.1854
All	-0.0909	-0.5815	649.1205	0.1476

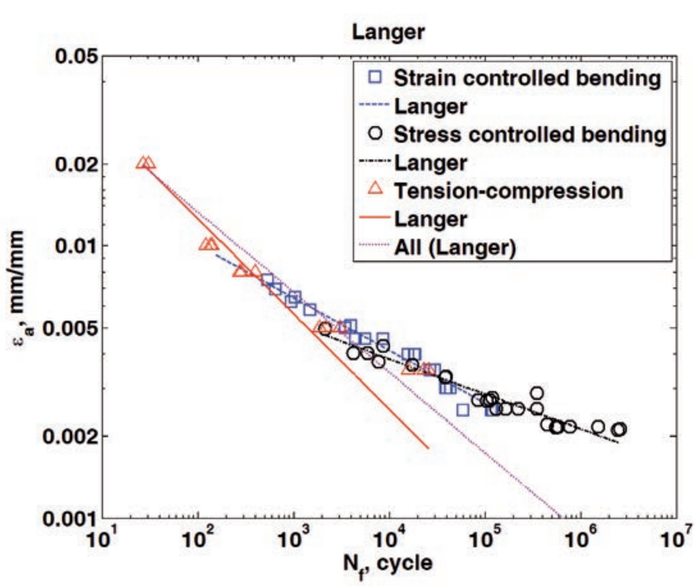

Fig. 12. Fatigue characteristics according to the Langer model

Table 10. Comparison of parameters of the analysed characteristics according to the Langer model

Langer				
	A	*B*	*C*	R^2
bending (stress controlled)	-1.898	0.1292	0.002	0.9415
bending (strain controlled)	-1.611	0.1932	1.068	0.9796
Tension-compression	-1.2	0.3498	0.002	0.9629
All	-1.284	0.2952	0.2	0.9299

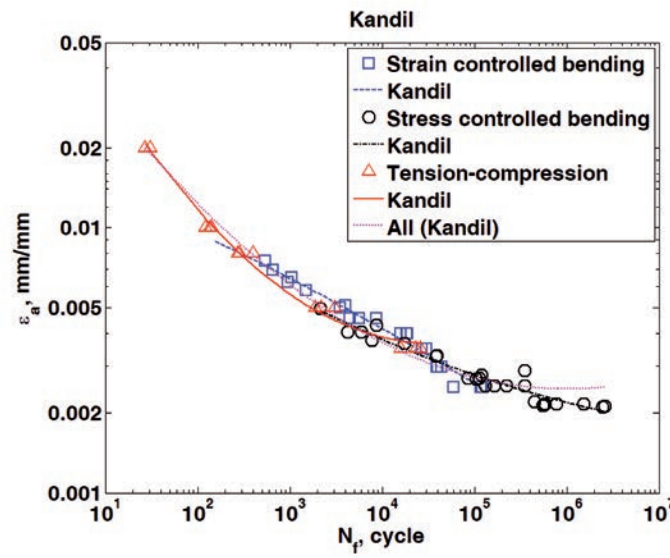

Fig. 13. Fatigue characteristics according to the Kandil model

Table 11. Comparison of parameters of the analysed characteristics according to the Kandil model

Kandil				
	A	*B*	*C*	R^2
bending (stress controlled)	-1.571	0.2738	0.01541	0.9501
bending (strain controlled)	-1.72	0.1321	-0.00823	0.9803
Tension-compression	-0.8345	0.7033	0.7033	0.9939
All	-1.035	0.5238	0.04359	0.9868

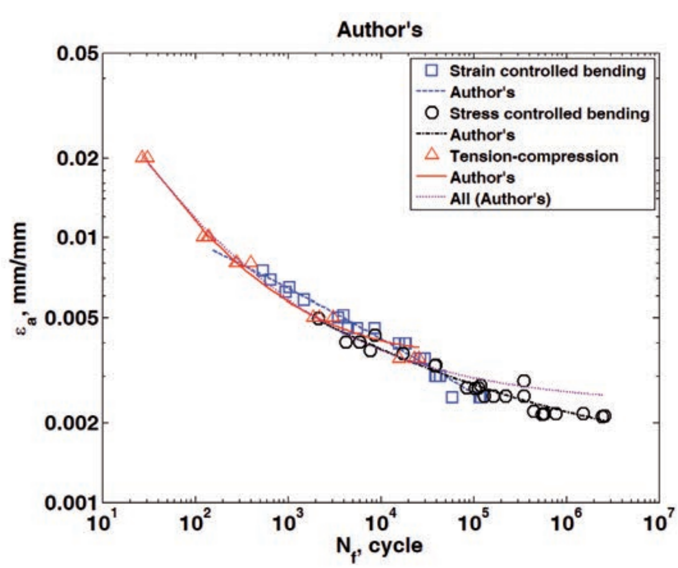

Fig. 14. Fatigue characteristics according to the model proposed by the Authors

Table 12. Comparison of parameters of the analysed characteristics according to the model proposed by the Authors

Authors'					
	a	***b***	***c***	***d***	R^2
bending (stress controlled)	-1.572	0.2704	0.01584	-0.0001774	0.9501
bending (strain controlled)	-1.709	0.1361	-0.006454	-0.0002348	0.9804
Tension-compression	-0.7877	0.761	0.07873	0.001406	0.994
All	-0.965	0.5946	0.03819	0.001919	0.9881

Conclusions

Experimental tests carried out for test pieces made of 6082-T6 aluminium alloy under strain control in conditions of single-axis tension-compression, and both under strain control and moment control for oscillatory bending, are much the same and independent of the loading method.

The tests under controlled strain may be replaced by oscillatory bending carried out on a simple, modern test bench instead of the basic tension-compression test performed using large fatigue-testing machines.

The best known Mason-Coffin-Basquin strain characteristic describes the results of all experimental tests very well; however, it can be used only when there is a possibility to divide strains into elastic and plastic components.

The Langer strain characteristic describes fatigue test results incorrectly, and it is not recommended for use to characterise fatigue test results.

The best match of fatigue characteristic to all experimental data is ensured by the four-parameter characteristic proposed by the authors, which is a fragment of a parabola in a double-logarithmic system, and it is slightly better than the three-parameter Kandil characteristic.

Acknowledgements

This work has been carried out under the grant of National Science Centre (Poland) no. 2015/19/B/ST8/01115.

References

1. Kurek A., Koziarska J., Kluger K., Łagoda T.: Fatigue life of 2017-T4 aluminium alloy under different types of stress. Journal of Machine Construction and Maintenance, 2017, 4, pp. 53–61.
2. Kurek M., Łagoda T., Walat K.: Variations of selected cyclic properties depending on testing temperature. Material Science, 2015, 50(4), pp. 555–563.
3. Kurek M., Łagoda T., Katzy D.: Comparison of fatigue characteristics of some selected materials. Material Testing, 2014, 56(2), pp. 92–95.
4. Walat K., Łagoda T., Kurek M.: Life time assessment of an aluminum alloy under complex low cycle fatigue loading. Material Testing, 2015, 57(2), pp. 160–164.
5. Manson S.S., Muralidharan U.: Fatigue life prediction in bending from axial fatigue information. Fatigue & Fracture Engineering Materials & Structures, 1987, 9(5), pp. 357–372.
6. Kulesa A., Kurek A., Łagoda T., Achtelik H., Kluger K.: Comparison of 15Mo3 strain curves obtained for strain-controlled cyclic bending and tension-compression tests. Solid State Phenomena, 2016, 250, pp. 85–93.
7. Troschenko V.: High-cycle fatigue and Inelasticity of Metals. In: Pinueau A., Cailletaud G., Lindley T.C. (eds.): Multiaxial Fatigue and Design (ESIS 21). London: Mechanical Engineering Publications, 1996, pp. 335–348.
8. Megahed M.M.: Prediction of bending fatigue behaviour by the reference stress approach. Fatigue & Fracture of Engineering Materials & Structures, 1990, 13(4), pp. 361–374.
9. Krzyżak D., Kurek M., Łagoda T., Sówka D.: Influence of changes of the bending plane position on the fatigue life. Materialwissenschaft und Werkstofftechnik, 2014, 45(11), pp. 1018–1029.
10. Basquin O.H.: The exponential law of endurance tests. American Society for Testing and Materials Proceedings, 1910, 10, pp. 625–630.
11. Coffin L. F.: A study of the effect of cyclic thermal stresses on a ductile metal. Trans ASME, 1954, 76, pp. 931–950.
12. Manson S.S.: Fatigue: a complex subject - some simple approximation. Experimental Mechanics, 1965, 5, pp. 193–226.
13. Marcisz E., Niesłony A., Łagoda T.: Concept of fatigue for determining characteristics of materials with strengthening. Material Science Forum, 2012, 726, pp. 43–48.
14. Radhakrishnan V.M.: On bilinearity of Manson-Coffin low-cycle-fatigue relationship. NASA Technical Memorandum, NASA-TM-105840, E-7283, WU-553-13-00, 1992.

15. Ramberg W., Osgood W.R.: Description of stress--strain curves by three parameters. Technical Note No. 902. Washington: National Advisory Committee for Aeronautics, 1943.
16. Langer B.F.: Design of Pressure Vessels for Low--Cycle Fatigue. Journal of Basic Engineering, 1962, pp. 389–402.
17. Manson S.S: Inversion of the strain-life and strain--stress relationships for use in metal fatigue analysis. Fatigue of Engineering Materials and Structures, 1979, 1, pp. 37–57.
18. Chopra O.K.: Effects of LWR coolant environments of fatigue design curves of austenitic stainless steels. U.S. Nuclear Regulatory Commission, 1999.
19. Kandil F.A.: The Determination of Uncertainties in Low Cycle Fatigue Testing. Standards Measurement & Testing Project No. SMT4-CT97-2165, 2000, 1, pp. 1–26.
20. Gorash Y., Chen H.: On creep-fatigue endurance of TIG-dressed weldments using the linear matching method. Engineering Failure Analysis, 2013, 34, pp. 308–323.
21. Niesłony A., Kurek A., EL Dsoki Ch., Kaufmann H.: A Study of Compatibility Between two Classical Fatigue Curve Models based on Some Selected Structural Materials. International Journal of Fatigue, 2012, 39, pp. 88–94.
22. Niesłony A., Kurek A.: Influence of the selected fatigue characteristics of the material on calculated fatigue life under variable amplitude loading. Applied Mechanics and Materials, 2012, 104, pp. 197–205.
23. Mroziński S.: Wyznaczanie własności niskocyklowych stopu aluminium PA4 w temperaturze otoczenia. Raport z badań. Bydgoszcz: UTP, 2012 (in Polish).
24. Kulesa A., Kurek A., Łagoda T., Achtelik H., Kluger K.: Low cycle fatigue of steel in strain controlled cyclic bending. Acta Mechanica et Automatica, 2016, 10(1), pp. 62–65.